













RE-EXPLORING THE RADIO SPECTRUM OF URANUS IN ORBIT: SCIENCE CASE AND DIGITAL HIGH FREQUENCY RECEIVER

L. Lamy^{1,2*} , B. Cecconi¹ , M. Dekkali¹ , P. Zarka¹ ,
C. Briand¹ , M. Moncuquet¹ , F. Pantellini¹ , L. Griton¹ ,
A. Boudouma¹ , X. Bonnin¹ , P.-L. Astier¹, D. Dias¹,
V. Gamage¹, B. Collet² , and C. K. Louis³ 

*Corresponding author: Laurent.Lamy@obspm.fr

Citation:

Lamy et al., 2023, Re-exploring the radio spectrum of Uranus in orbit: science case and digital high frequency receiver, in *Planetary, Solar and Heliospheric Radio Emissions IX*, edited by C. K. Louis, C. M. Jackman, G. Fischer, A. H. Sulaiman, P. Zucca, published by DIAS, TCD, pp. 407–420, doi: 10.25546/103105

Abstract

Among the known planetary magnetospheres, those of Uranus and Neptune display very similar radio environments so that they were referred to as radio twins. Their pioneering exploration by the Voyager 2 Planetary Radio Astronomy (PRA) and Plasma Wave Science (PWS) experiments revealed a variety of electromagnetic radio waves ranging from a few kHz to a few tens of MHz similar to - although more complex than - those of Saturn or the Earth. The asymmetric magnetosphere of Uranus is highly atypical with a large obliquity, magnetic tilt and fast rotation period, so that the magnetosphere undergoes perpetual geometric reconfiguration. Hereafter, we review the rich zoo of Uranian radio emissions, including the auroral Uranian Kilometric Radiation (UKR) between a few kHz and 1 MHz, the Uranian Electrostatic Discharges (UED) observed up to 40 MHz, and low frequency waves (continuum, plasma wave emissions) at a few kHz. We then emphasize the interest of re-exploring this atypical radio source and present a modern concept of a digital High Frequency Receiver (HFR) in the framework of a Radio and Plasma Wave (RPW) experiment to be proposed to any future NASA/ESA orbital mission toward

¹ LESIA, Observatoire de Paris, Université PSL, CNRS, Sorbonne Université, Université de Paris, Meudon, France

² Aix Marseille Université, CNRS, CNES, LAM, Marseille, France

³ School of Cosmic Physics, DIAS Dunsink Observatory, Dublin Institute for Advanced Studies, Dublin 15, Ireland

Uranus. This HFR concept, updated from the heritage of Cassini/RPWS/HFR, STEREO/Waves, Bepi-Colombo/PWI/Sorbet or Solar Orbiter/RPW is aimed at providing a light, robust, low-consumption versatile instrument capable of goniopolarimetric (polarization and direction-finding capabilities) and waveform measurements from a few kHz to ~ 40 MHz, devoted to the study of radio emissions, plasma waves and dust impacts.

1 Introduction

The Voyager 2 spacecraft flew by Uranus in 1986, with a closest approach on 24th Jan. At this occasion, its Planetary Radio Astronomy (PRA) and Plasma Wave Science (PWS) remote sensing experiments acquired pioneering radio measurements over the 1.2 kHz–40 MHz and 10 Hz–56.2 kHz spectral ranges, respectively. PRA scanned its high frequency band with 200 channels in 6 seconds using two 10-m long orthogonal electric monopole antennas to measure the wave flux density and apparent Left- or Right-Handed (LH or RH) sense of circular polarization (Warwick et al., 1977). PWS survey observations scanned the low frequency band with 16 channels every 4 seconds, using both antennas in dipole mode (Scarf & Gurnett, 1977) to sense flux densities. Both instruments revealed an unexpectedly rich radio spectrum (Warwick et al., 1986). These include the Uranian Kilometric Radiation (UKR) between a few kHz and 1 MHz produced in the auroral regions, the Uranian Electrostatic Discharges (UEDs) above 1 MHz which probe atmospheric lightnings together with low frequency emissions below 60 kHz diagnosing various magnetospheric plasma wave phenomena (Desch et al., 1991; Farrell, 1992). Only Neptune, similarly observed by Voyager 2 three years later, displayed similar, although fainter, radio emissions, so that both radiosources were considered as radio twins. In this article, we briefly review our current understanding of the Uranian radio spectrum (Section 2) and the need for re-exploring it in a different magnetospheric configuration (Section 3) before presenting a novel concept of digital high frequency receiver in the framework of a radio and plasma wave instrument aboard any future Uranus orbiter (Section 4).

2 Uranus as a radio source

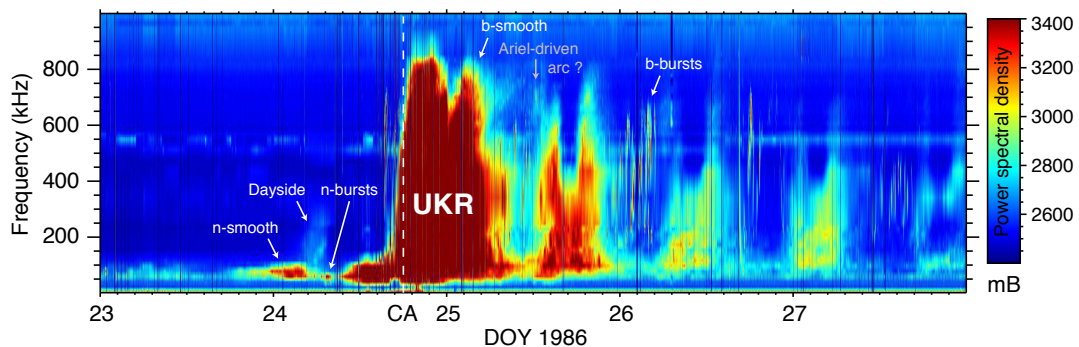
Out of an early tentative detection of Uranus at ~ 500 kHz with IMP-6 from Earth in the early 1970s (Brown, 1976), our knowledge of non-thermal radio emissions of Uranus entirely relies on Voyager 2 PRA/PWS observations, that detected 8 distinct radio components (listed in Table 1) probing various regions of the magnetosphere and the atmosphere. These were reviewed in depth by Desch et al. (1991); Farrell (1992); Zarka (1998) and their main characteristics are summarized below.

Table 1: Family portrait of the Uranian radio emissions. *N* and *S* stand for Northern and Southern.

Components	Spectrum	Polar.	Mode	Variability	Source	Generation
UED	1-40 MHz	-	free space	~ min-hours	Atmosphere	Lightnings
UKR b-smooth	150-900 kHz	LH	R-X	rotation	S magn. pole	CMI
UKR n-smooth	20-350 kHz	RH/LH	R-X	rotation	Magn. equator	
UKR dayside	100-300 kHz	LH	L-O	rotation	N magn. pole	
UKR b-bursts	200-800 kHz	LH	R-X	rotation, 30 Hz	S magn. pole	
UKR n-bursts	15-120 kHz	RH	R-X	solar wind	N cusp?	
Continuum	≤6 kHz	RH	L-O	rotation	Magn. equator	es/em
5 kHz noise	3-10 kHz	?	?	-	Miranda	es/em

2.1 Uranian kilometric radiation

UKR is the most powerful Uranian radio emission, reminiscent of the Terrestrial and Saturnian Kilometric Radiations (TKR and SKR, resp.) and, to a lesser degree, to Jovian kilometric (b-KOM, b standing for broadband) to decametric (DAM) auroral radio emissions. It was thus early thought to be similarly produced near the electron gyrofrequency f_{ce} by the Cyclotron Maser Instability (CMI). The latter is driven by energetic electrons in magnetized, tenuous regions where f_{ce} is much higher than the electron plasma frequency f_{pe} . UKR was observed to be highly circularly polarized with a spectrum ranging from 15 to 850 kHz which strikingly compared to that of TKR/SKR, although typically fainter by an order of magnitude. UKR was additionally mainly beamed toward the nightside of the magnetosphere, so that it could only be detected during a restricted time interval spanning from 5 days before the closest approach (CA) until 1 month after. Figure 1 displays a 5-days long dynamic spectrum of UKR near the CA.

**Figure 1:** Voyager 2/PRA time-frequency observation of Uranus near the CA in Jan. 1986. The various UKR components are labelled individually.

Overall, UKR can be sub-divided in 5 components, either narrowbanded or broadbanded (n- or b-), radiated from both magnetic poles either on the extraordinary (X or R-X, where R stands for right-handed) or Left-Handed Ordinary (O or L-O, where L stands for left-handed) oblique wave propagation mode in a magnetized medium. They also decompose into (i) bursty emissions with temporal duration ≤ 10 min, as commonly observed at Earth, Jupiter and Saturn and (ii) smooth emissions that are time-stationary for hours and uniquely observed at Uranus and Neptune. PRA observations were used to infer the

locus of UKR sources, their beaming and polarization state, although with significant differences resulting from the assumptions made to invert the 2-antenna measurements, *e.g.* (Sawyer et al., 1991). Figure 2 summarizes the inferred magnetic flux tubes hosting the UKR sources (left) and their ionospheric footprint (right).

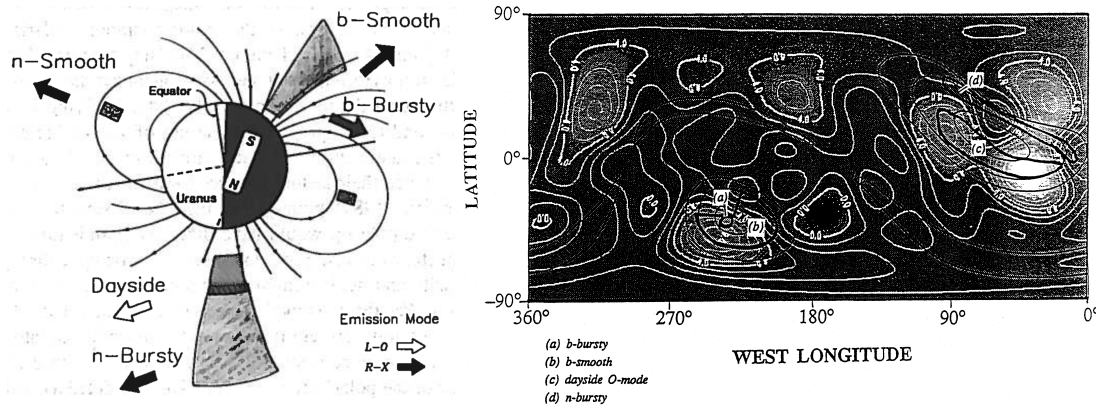


Figure 2: (Left) Locus of the UKR sources (Desch et al., 1991). (Right) Cylindrical map of the UKR magnetic footprints on top of the UV auroral intensity, from Farrell (1992).

2.1.1 Smooth emissions

The b-smooth emission (also sometimes referred to as Smooth High Frequency or SHF) was the prominent UKR component, radiating $\sim 10^7$ W, and regularly observed every ~ 17 h for days after the CA. It was found to propagate on the X mode from southern magnetic flux tubes mapping to $L = 20$ to 30 Uranian radii (R_U), near the boundary between open and closed field lines ($L \sim 18$) and restricted to an active sector of longitude, although variable results have been published in the literature *e.g.* Kaiser et al. (1987); Leblanc et al. (1987); Zarka & Lecacheux (1987); Lecacheux & Ortega-Molina (1987); Gulkis & Carr (1987). This area partially overlaps with the southern UV auroral region and the polar cap (Figure 2). The b-smooth beaming was identified as a thick-walled hollow conical sheet with a 50° aperture with respect to $-B$ (Zarka & Lecacheux, 1987). Its stable repeatable dropouts (high frequency extinctions) were used to derive a rotation rate of 17.24 ± 0.01 h (Desch et al., 1986), while the observed scintillations were attributed to the wave activity of the magnetopause. The b-smooth steady-state and high flux density intensity requires a constant CMI-unstable source of free energy. Several candidates, such as the dayside plasmasphere (Curtis et al., 1987) or the moon Miranda (Romig et al., 1987), have been debated.

The so-called dayside component is a weak, smooth, emission radiated from the dayside above the northern magnetic pole along field lines possibly colocated with the nightside sources of b-smooth. It has been identified to propagate on the O mode (Desch & Kaiser, 1987), which makes it the only known auroral planetary radio component with a prominent O mode polarization. CMI can account for a direct and preferential O mode emission in regions where the density is high and the f_{pe}/f_{ce} ratio is close to unity (Menietti & Curran, 1990).

The n-smooth component (also sometimes referred to as Smooth Low Frequency or SLF) is a narrowbanded ($\delta f/f \sim 0.5$) X mode emission, continuous over hours (Leblanc et al., 1987). It has been observed both on the inbound and outbound encounter periods, with an amplitude varying as a function of the rotational phase, while changing polarization sense from RH to LH at the magnetic equator crossing. It was proposed to be driven by the CMI near the magnetic equator region, suggesting that the latter contains a sufficiently tenuous plasma (Kaiser et al., 1989; Sawyer et al., 1991), prevented to accumulate near the equatorial plane due to the magnetic tilt combined with the rotation. The existence of a planetary auroral radio emission originating from the magnetic equator had never been observed before, and was only similarly seen on Neptune, which would be another property unique to the ice giants' magnetospheres.

2.1.2 Bursty emissions

Among the bursty emissions, the n-burst component consisted of narrowbanded ($\delta f/f \sim 0.1$) X mode emission, above the northern magnetic pole (L-shell ranging from 4 to 11 R_U , corresponding to closed field lines at the low latitude edge of the northern polar cusp) with a ~ 250 ms duration (Gurnett et al., 1986; Desch et al., 1989). This was the dominant dayside component with a total radiated power of about $\sim 10^6$ W. The origin of individual bursts remains unknown, but their long-term occurrence appeared to correlate with the solar wind density. We note that a solar wind forcing mediated by bursty dayside magnetic reconnection would be consistent with a cusp source region and in agreement with the localized transient UV auroral spots recently observed by HST on the dayside (Lamy et al., 2012).

b-bursts correspond to intense broadband impulsive X mode emissions, lasting from 2 to 10 min (Warwick et al., 1986; Leblanc et al., 1987; Evans et al., 1987; Kaiser et al., 1987). Like the b-smooth component, these emissions were emitted near the nightside southern magnetic pole, from a restricted sector of longitudes, and modulated at the planetary rotation period. But unlike b-smooth, the emission was beamed at higher angles ($\sim 80^\circ$) from the local magnetic field vector. b-burst decomposed into periodic bursts lasting a few 10 ms with a 30 Hz period, related to the ion density perturbations in the source region. Some high frequency arc-structures, observed between 600 and 800 kHz for 3 h with a 10 min periodicity (and sometimes proposed to form a different radio component) were proposed to be triggered by some Ariel-Uranus alfvénic interaction (Kistler, 1988). Such an interaction is expected to be highly dynamic, as the moon experiences a wide range of magnetic conditions along its orbit. The re-analysis of these arcs to check their origin is the purpose of a companion study (Louis et al., 2023, this issue).

2.2 Uranian electrostatic discharges

Near the CA, within 20 R_U from Uranus, PRA revealed a cluster of impulsive high frequency bursts between 1 and 40 MHz, reminiscent of the radio signature of atmospheric lightnings well known at Earth and previously observed by PRA at Saturn. These were termed thus UED by analogy with Saturn Electrostatic Discharges (SED) and analyzed

in depth by Zarka & Pedersen (1986). As for SED, such bursts had a lifetime shorter than a complete scan of the PRA band, so that they appeared in a small series of frequency channels despite their spectrum being broadband, as illustrated in Figure 3, left. About 140 UED were unambiguously detected with a 120 ms average duration. They occurred in episodes lasting from a few min to a few hours, but without any long-term periodicity, which prevented one to localize their source region. Above a few MHz, the UED spectrum displayed in Figure 3, right roughly decreases in $1/f^2$, like at Earth, but unlike at Saturn where the SED spectrum varies in $1/f$. The UED instantaneous power radiated over the entire observed spectrum reaches 10^8 W, 10 times lower than SED. Fewer and weaker events than observed at Earth or Saturn could result from a lower level of atmospheric convective motion and low polarizable atmospheric molecules (methane vs *e.g.* ammonium observed at Saturn) involved in lightning generation. The UED low frequency cutoff, which relates to the ionospheric cutoff, evolved from 7 MHz on the dayside to 900 kHz on the nightside. These values yielded a dayside and nightside sub-spacecraft peak ionospheric electron density of 6×10^5 and 10^4 cm^{-3} , respectively, in agreement with radio science results. The long-term monitoring of UED would provide a high value-added proxy on the atmospheric and ionospheric conditions but, despite numerous attempts, they have never been re-detected remotely (either from space or from the ground).

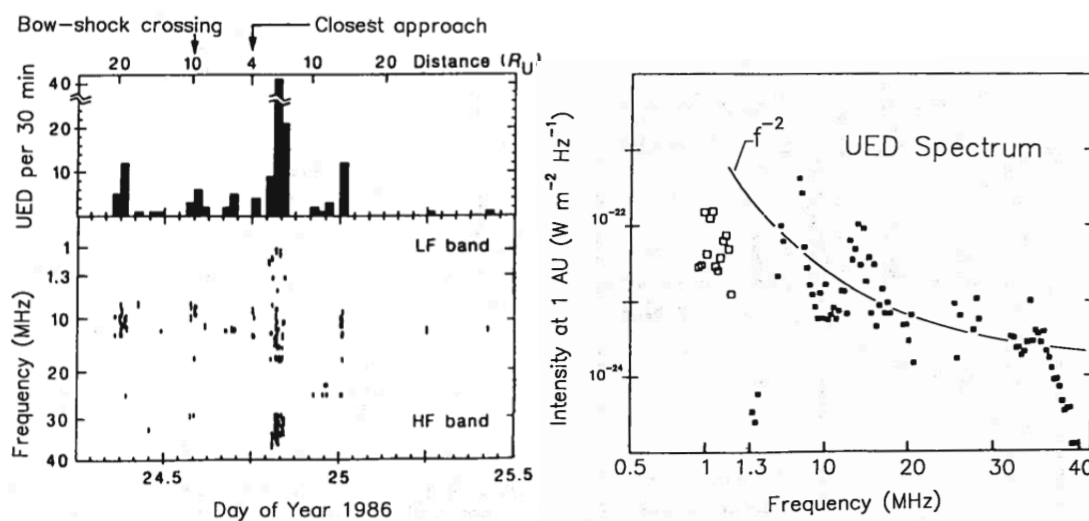


Figure 3: (Left) Dynamic spectrum, temporal occurrence and (Right) spectrum of UED (Zarka & Pedersen, 1986; Desch et al., 1991).

2.3 Low frequency radio emissions

In the low frequency range, a continuum radiation was detected by PWS and PRA between 1 and 3 kHz with a diffuse extension beyond 6 kHz. It was detected at the magnetopause crossing, persisting for at least 2 h. and observed to be RH polarized, consistent with O mode propagation. This component is reminiscent of the non-thermal continuum radiation ubiquitously observed at Earth, Jupiter and Saturn. It was proposed to be produced in the density cavity between the magnetopause and the inner magnetosphere from intense

electrostatic waves observed near the magnetic equator at the upper hybrid frequency and then affected by successive mode conversion to Z and O free-space mode (Kurth et al., 1990).

Finally, PWS also detected narrowbanded 5 kHz bursts between 3 and 10 kHz (undetectable to PRA as these fell within 2 frequency channels), varying at timescales of 1 s. Such emissions were mostly observed along the outbound leg of the spacecraft flyby and as far as $\sim 600 R_U$. This component was suspected to be produced near the Miranda L-shell from mode conversion involving intense electrostatic noise, but the nature of the mode conversion mechanism and the origin of the emission sporadicity is unknown (Kurth et al., 1986).

3 The need for re-exploring the Uranus radio spectrum

3.1 A unique radio emitter

Uranus stands with Neptune as the archetype of asymmetric magnetospheres and the large inclination of its spin axis makes its upper atmosphere subject to long term solar insolation unique in the solar system. In the solstice configuration probed by Voyager 2, Uranus appeared as an unexpectedly rich radio emitter when compared to the Earth or Saturn, as complex as Jupiter. PRA/PWS measurements yielded a pioneer characterization of UKR, UED and low frequency radio emissions and revealed unique characteristics either shared with Neptune or unique to Uranus. However, the instrumental limitations of PRA/PWS experiments (2-antenna measurements, low time-frequency resolution) coupled to the restricted dataset collected along the Voyager 2 flyby prevented one from achieving a comprehensive picture of these radio components. For instance, it remained unclear why UKR was only weakly driven by the solar wind, as opposed to the Earth or Saturn, while the Uranian magnetosphere is expected to be particularly sensitive to it (see e.g., Tóth et al., 2004; Cao & Paty, 2017; Griton et al., 2018; Pantellini, 2020). The source and polarization state of UKR components was poorly constrained and their free energy source is not yet understood. The limited number of detected UED only provided preliminary informations onto atmospheric storms and ionospheric peak density.

Farrell (1992) already pointed out the need for an in-depth exploration of this radio emitter. Unless using a sensitive enough radiotelescope from the farside of the moon (Zarka et al., 2012) (which would be limited to the remote monitoring of dayside radio components), re-observing the radio spectrum from Uranus requires a dedicated exploration probe equipped with a modern, sensitive, Radio and Plasma Wave (RPW) experiment. Such an instrument and the broad science case it would address have already been detailed in several missions concepts proposed to explore the Uranian system (see e.g., Arridge et al., 2023, and refs therein). The experience of 13 years of observations of Saturn by Cassini/RPWS in orbit yielded a rich, sometimes unexpected, scientific return and high value-added to the original Voyager flyby.

The solar wind/magnetosphere configuration, and associated plasma transport and acceleration processes, additionally strongly evolve along the Uranus' revolution (Ness et al.,

1991). Highly variable UV aurorae have been detected from Earth past the equinox of 2007, a configuration during which the magnetosphere reorganizes itself from a pole-on to an Earth-like configuration four times per rotation (Lamy et al., 2017). While a future Uranus orbiter is now under discussion, any promptly selected and constructed spacecraft would reach the planet in the 2040s at best. The time interval ranging from the solstice of 2028 (where the strong-field southern magnetic pole will permanently lie on the dayside) to the equinox of 2049 corresponds to unknown magnetospheric configurations yet to be probed in situ which could reveal completely new and intense components. It is finally not only essential to deepen our understanding of Uranus radio emissions in the context of comparative planetology but also in the framework of the ongoing radio search for exoplanets, a large part of which are Uranus-class planets (Fulton & Petigura, 2018).

3.2 Objectives of a future radio experiment

A radio experiment onboard any future Uranus orbiter should perform value-added measurements with respect to Voyager 2/PRA and PWS, improving the instrumental sensitivity, the time-frequency resolution and providing the full set of Stokes parameters of radio waves between a few kHz and a few tens of MHz to sample adequately all the radio components of Table 1. Long enough radio antennas proved to be a valuable tool to probe plasma parameters and/or micrometer-sized dusts impacting the spacecraft. Finally, the large magnetic tilt of the planet will facilitate the in situ exploration of auroral radio sources and acceleration regions, such as for Cassini and Juno.

Such an experiment would be necessary to address questions such as : What is the internal rotation rate? What is specific to the Ice giant auroral radio emissions? How are they produced? What is the source of free energy driving their unique smooth components? What is the origin of bursts, there as elsewhere? What makes the Uranian magnetic equator an auroral radio emission region? What is the overall magnetospheric configuration? What are the relative roles of rotation, solar wind and moons in driving magnetospheric dynamics and particle acceleration processes? What makes the specificity of ice giant lightnings? How does the ionosphere vary with time? How are dusty rings structured and how do they evolve?

Additional cruise phase objectives could include the remote monitoring of radio emissions of Jupiter and/or Saturn from long distances and of solar radio emissions/local plasma waves and dust impacts in the heliosphere.

4 A broadband digital high frequency receiver

4.1 A digital concept

The LESIA laboratory has a long history in designing and building sensitive radio receivers with goniopolarimetric (polarization and direction-finding) capabilities such as Ulysses/URAP, WIND/Waves, STEREO/Waves, Cassini/RPWS/HFR and, most recently, Bepi-Colombo/MIO/PWI/Sorbet and Solar Orbiter/RPW.

Building on this heritage, the LESIA laboratory recently developed a novel concept of a fully digital receiver through the PERLS (Plateforme d’Evaluation Radio-Logicielle Spatiale) research and development program supported by the CNES french space agency. This receiver is based on the latest rad-hardened technologies : using Software Defined Radio (SDR) concepts, it is widely reconfigurable to tackle a variety of scientific cases. Overall, it consists of (i) hardware, which includes analog radio frequency front end, high-speed 16-bit digitizers, and digital infrastructure, (ii) VHDL firmware supporting (VHDL stands for Very High Speed Integrated Circuit Hardware Description Language), along with the processor, data acquisition and digital signal processing accelerators and (iii) on-board software covering TM/TC (telemetry and telecommand) management, task scheduler, high-level processing and data reduction. Thanks to sophisticated on-board processing and optimized implementation, this analyzer can cover a wide spectral range from a few kHz to at least 40 MHz for 16-bit coded signals. The receiver can deliver a variety of data products, such as snapshots of waveforms at different sampling rates, spectral matrices including correlations, as well as wavelet analysis. These products can easily be supplemented with other in-flight treatments.

As of today, two successive PERLS receiver prototypes have already been built and tested in the laboratory, so that the Technology Readiness Level is about 4-5. The testing phase will take advantage of radio antennas of the Nançay Decameter Array to perform physical data acquisition of solar and jovian radio emissions between 5-10 (terrestrial ionospheric cutoff) and 40 MHz. PERLS receivers are considered for various space probes under study, such as the CIRCUS nanosat or the Plasma Observatory ESA-M7 mission concepts.

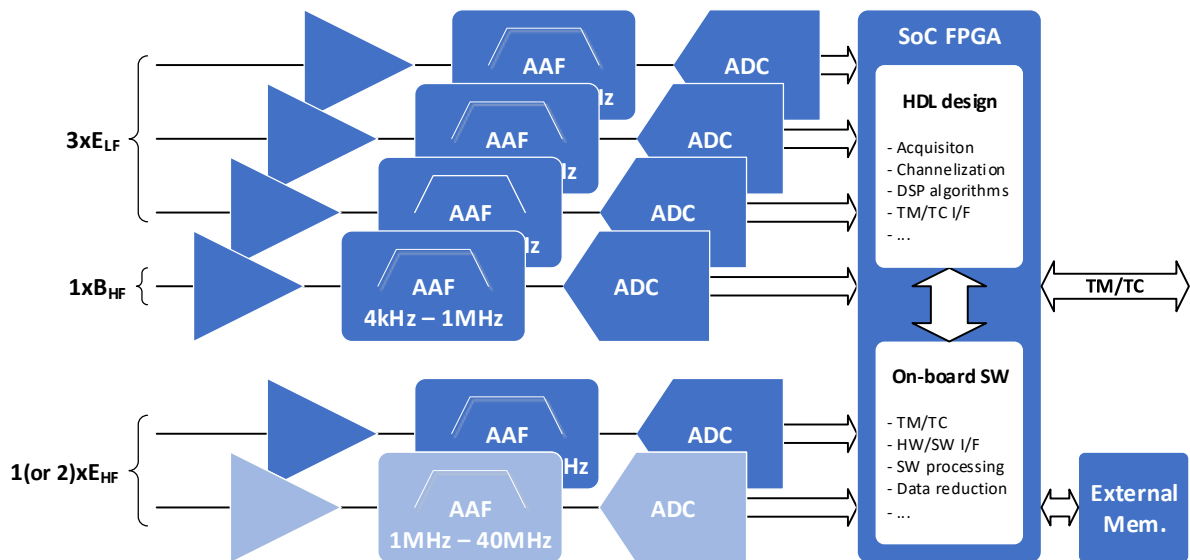


Figure 4: Block diagram of the proposed digital HFR receiver. The top (bottom) part refer to low frequency (high frequency) measurements involving 3 electric sensors + 1 magnetic sensor in option (1 or 2 electric sensors). Each line refers to a channel of the receiver, where the sensed signal is pre-amplified, anti-aliasing filtered (AAF), converted by a multi-channel analog-to-digital converter (ADC). The recorded signals are sent to and processed by a System on Chip (SoC) Field Programmable Gate Array (FPGA), including Digital Signal Processing (DSP), which ultimately delivers the needed products.

4.2 A HFR adapted for a Uranus orbiter

To fulfill the scientific goals of a radio experiment onboard a future orbital (spinning or 3-axes stabilized) probe while minimizing constraints, we need a light, robust, low-consumption, versatile instrument capable of goniopolarimetric and waveform measurements from a few kHz to ~ 40 MHz, devoted to the study of radio emissions and plasma waves of Uranus (and of the heliosphere) and of dust impacts. We therefore adapted the above-described concept of analyzer to achieve the High Frequency Receiver (HFR) displayed in Figure 4, which would sample the spectral ranges below and above 1 MHz with different measurement types, improving those collected by PRA/PWS, starting with a high (120 dB) dynamic range.

The low frequency band, ranging from a few kHz to 1 MHz and dealing with the UKR, the continuum and the 5 kHz noise, would highly benefit from the full determination of the Stokes parameters from auto- and cross-correlation time-frequency/waveform measurements between at least 3 sensors (assuming a baseline of 3 electric antennas) and ideally 4 (with the option of 1 additional magnetic search coil). Another improvement with respect to PRA would be to achieve a finer spectral resolution enabling to sample the galactic background and to mitigate RFI efficiently.

The high frequency band, ranging from 1 MHz to 25 MHz and thus overlapping the range of UEDs and solar/jovian radio emissions, could be more simply sampled by two electric sensors, providing the opportunity to perform simple goniopolarimetric analysis depending on the antenna beaming pattern. An alternate option could be to restrict to a single electric measurement extending up to 40 MHz.

In this framework, the detailed HFR characteristics would be :

- Spectral range : 5 kHz to 40 MHz, covered by two bands
- Bands/sensors :
 - * Low band 3 kHz–1 MHz (UKR, LF waves) : 3 E baseline (+1 B in option)
 - * High band 1–25-40 MHz (UED, Jupiter, Sun) : 2E until 25 MHz or 1E until 40 MHz
- Direct digitization : 16 bits-ADC with a 120 dB dynamic range
- Performances : t-f mode with full auto-/cross-correlations (3-antenna goniopolarimetry ≤ 1 MHz), waveform capture (5 Msps / channel ≤ 1 MHz)
- Size : 160x240x25- mm (1 PCB board)
- Weight : 500 g excluding harnesses and electronic box
- Power : 3.5 W in average + 0.6 W (for 3 pre-amplifiers)
- Telemetry : typical rate of a few kbps
- Heritage : Cassini/RPWS/HFR, Bepi-Colombo/PWI/Sorbet, Solar Orbiter/RPW, R&D CNES PERLs program

- Technology Readiness Level : 6 in 2024

Experience acquired with the above-mentioned radio receivers, together with the investment of our team in JUICE/RPWI/JENRAGE (in which we are involved for the data acquisition and distribution) will help to minimize the telemetry rate by exploiting operational modes, data onboard storage and compression. Maturation of the TRL level is ongoing and should reach 6 within 2 years.

5 Conclusions and perspectives

The pioneering exploration of Uranus by Voyager 2 revealed an unexpectedly rich radio emitter with a variety of electromagnetic radio waves ranging from a few kHz to a few tens of MHz probing the auroral and equatorial magnetospheres, together with the upper atmosphere. We have reviewed their characteristics and highlighted those unique to Uranus and Neptune as Ice giant planetary systems or to Uranus alone. The single flyby of Voyager 2, in the particular solar wind/magnetosphere configuration which prevailed at solstice did not yield a comprehensive view of the Uranian emissions, both remotely and in situ. A re-exploration of the Uranian radio spectrum is required to deepen our understanding of these, both in the context of comparative planetology but also in the framework of the ongoing radio search for exoplanets. In the context of a future Uranus orbiter equipped with a Radio and Plasma Wave dedicated experiment, we propose a light, robust, low-consumption, versatile High Frequency Receiver capable of goniopolarimetric and waveform measurements from a few kHz to ~ 40 MHz with 3 antennas, devoted to the study of radio emissions, plasma waves and dust impacts.

Acknowledgements

The authors thank both referees for their valuable and constructive comments and acknowledge support from CNES and from CNRS/INSU programs of Planetology (PNP) and Heliophysics (PNST). C. K. Louis' work at the Dublin Institute for Advanced Studies was funded by the Science Foundation Ireland Grant 18/FRL/6199.

References

- Arridge C. S., et al., 2023, Fundamental Space Physics in Uranus' Magnetosphere, *in Bulletin of the American Astronomical Society*, p. 018, doi:10.3847/25c2cf2023.15e9f2c8
- Brown L. W., 1976, Possible radio emission from Uranus at 0.5 MHz., *The Astrophys. J.*, 207, L209
- Cao X., Paty C., 2017, Diurnal and seasonal variability of Uranus's magnetosphere, *Journal of Geophysical Research (Space Physics)*, 122, 6318

- Curtis S. A., Desch M. D., Kaiser M. L., 1987, The radiation belt origin of Uranus' nightside radio emission, *J. Geophys. Res.*, *92*, 15199
- Desch M. D., Kaiser M. L., 1987, Ordinary mode radio emission from Uranus, *J. Geophys. Res.*, *92*, 15211
- Desch M. D., Connerney J. E. P., Kaiser M. L., 1986, The rotation period of Uranus, *Nature*, *322*, 42
- Desch M. D., Kaiser M. L., Kurth W. S., 1989, Impulsive solar wind-driven emission from Uranus., *J. Geophys. Res.*, *94*, 5255
- Desch M. D., Kaiser M. L., Zarka P., Lecacheux A., Leblanc Y., Aubier M., Ortega-Molina A., 1991, Uranus as a radio source., in *Uranus*, eds Bergstrahl, Jay T. and Miner, Ellis D. and Matthews, Mildred S., pp 894–925
- Evans D. R., Romig J. H., Warwick J. W., 1987, Bursty radio emissions from Uranus, *J. Geophys. Res.*, *92*, 15206
- Farrell W. M., 1992, Nonthermal radio emissions from Uranus, in *Planetary Radio Emissions III*, pp 241–269
- Fulton B. J., Petigura E. A., 2018, The California-Kepler Survey. VII. Precise Planet Radii Leveraging Gaia DR2 Reveal the Stellar Mass Dependence of the Planet Radius Gap, *T. Astrophys. J.*, *156*, 264
- Griton L., Pantellini F., Meliani Z., 2018, Three-Dimensional Magnetohydrodynamic Simulations of the Solar Wind Interaction With a Hyperfast-Rotating Uranus, *Journal of Geophysical Research (Space Physics)*, *123*, 5394
- Gulkis S., Carr T. D., 1987, The main source of radio emission from the magnetosphere of Uranus, *J. Geophys. Res.*, *92*, 15159
- Gurnett D. A., Kurth W. S., Scarf F. L., Poynter R. L., 1986, First Plasma Wave Observations at Uranus, *Science*, *233*, 106
- Kaiser M. L., Desch M. D., Curtis S. A., 1987, The sources of Uranus' dominant nightside radio emissions, *J. Geophys. Res.*, *92*, 15169
- Kaiser M. L., Desch M. D., Connerney J. E. P., 1989, Radio emission from the magnetic equator of Uranus, *J. Geophys. Res.*, *94*, 2399
- Kistler A. C., 1988, Voyager 2 Detection of Uranian Hectometric Radio Arcs, https://space.physics.uiowa.edu/~dag/theses_docs/Kistler_MS_1988_r.pdf
- Kurth W. S., Gurnett D. A., Scarf F. L., 1986, Sporadic narrowband radio emissions from Uranus, *J. Geophys. Res.*, *91*, 11958
- Kurth W. S., Gurnett D. A., Desch M. D., 1990, Continuum radiation at Uranus, *J. Geophys. Res.*, *95*, 1103

- Lamy L., et al., 2012, Earth-based detection of Uranus' aurorae, *Geophys. Res. Lett.*, *39*, L07105
- Lamy L., et al., 2017, The aurorae of Uranus past equinox, *Journal of Geophysical Research (Space Physics)*, *122*, 3997
- Leblanc Y., Aubier M. G., Ortega-Molina A., Lecacheux A., 1987, Overview of the uranian radio emissions: Polarization and constraints on source locations, *J. Geophys. Res.*, *92*, 15125
- Lecacheux A., Ortega-Molina A., 1987, Polarization and localization of the Uranian radio sources, *J. Geophys. Res.*, *92*, 15148
- Louis C. K., Lamy L., Jackman C. M., Cecconi B., Hess S. L. G., 2023, Predictions for Uranus-moons radio emissions and comparison with Voyager 2/PRA observations, in *Planetary, Solar and Helispheric Radio Emissions IX*, eds Louis, C. K. and Jackman, C. M. and Fischer, G. and Sulaiman, A. H. and Zucca, P., DIAS and TCD, doi:10.25546/103106
- Menietti J. D., Curran D. B., 1990, Source of O mode radio emissions from the dayside of Uranus, *J. Geophys. Res.*, *95*, 15263
- Ness N. F., Connerney J. E. P., Lepping R. P., Schulz M., Voigt G.-H., 1991, The magnetic field and magnetospheric configuration of Uranus., in *Uranus*, eds Bergstrahl, Jay T. and Miner, Ellis D. and Matthews, Mildred S., pp 739–779
- Pantellini F., 2020, A physical model for the magnetosphere of Uranus at solstice time, *Astron. & Astrophys.*, *643*, A144
- Romig J. H., Evans D. R., Sawyer C. B., Schweitzer A. E., Warwick J. W., 1987, Models of Uranian continuum radio emission, *J. Geophys. Res.*, *92*, 15189
- Sawyer C. B., Neal K. L., Warwick J. W., 1991, Polarization model applied to uranian radio emission, *J. Geophys. Res.*, *96*, 5575
- Scarf F. L., Gurnett D. A., 1977, A Plasma Wave Investigation for the Voyager Mission, *Sp. Sci. Rev.*, *21*, 289
- Tóth G., Kovács D., Hansen K. C., Gombosi T. I., 2004, Three-dimensional MHD simulations of the magnetosphere of Uranus, *Journal of Geophysical Research (Space Physics)*, *109*, A11210
- Warwick J. W., Pearce J. B., Peltzer R. G., Riddle A. C., 1977, Planetary Radio Astronomy Experiment for Voyager Missions, *Sp. Sci. Rev.*, *21*, 309
- Warwick J. W., et al., 1986, Voyager 2 radio observations of Uranus, *Science*, *233*, 102
- Zarka P., 1998, Auroral radio emissions at the outer planets: Observations and theories, *J. Geophys. Res.*, *103*, 20159

Zarka P., Lecacheux A., 1987, Beaming of Uranian nightside kilometric radio emission and inferred source location, *J. Geophys. Res.*, *92*, 15177

Zarka P., Pedersen B. M., 1986, Radio detection of uranian lightning by Voyager 2, *Nature*, *323*, 605

Zarka P., et al., 2012, Planetary and exoplanetary low frequency radio observations from the Moon, *Planet. & Sp. Sci.*, *74*, 156